

The Aluminum Distribution and Translocation in Two Citrus Species Differing in Aluminum Tolerance

Han Zhang

Fujian Agriculture and Forestry University

Xin-yu Li

Fujian Agriculture and Forestry University

Mei-lan Lin

Fujian Agriculture and Forestry University

Ping-ping Hu

Fujian Agricultural University: Fujian Agriculture and Forestry University

Ning-wei Lai

Fujian Agriculture and Forestry University

Zeng-rong Huang (✉ hzipaul@126.com)

Fujian Agriculture and Forestry University <https://orcid.org/0000-0003-1975-7399>

Li-song Chen

Fujian Agriculture and Forestry University

Research article

Keywords: Citrus sinensis, Citrus grandis, Al toxicity, Al distribution, Al translocation, Cell wall

Posted Date: August 9th, 2021

DOI: <https://doi.org/10.21203/rs.3.rs-789821/v1>

License:   This work is licensed under a Creative Commons Attribution 4.0 International License.

[Read Full License](#)

Abstract

Background: Many citrus orchards of south China suffer from soil acidification, which induced aluminum (Al) toxicity. The Al-immobilization *in vivo* is crucial for Al detoxification. However, the distribution and translocation of excess Al in citrus species were not well illustrated.

Results: The seedlings of 'Xuegan' [*Citrus sinensis* (L.) Osbeck] and 'Shatianyou' [*Citrus grandis* (L.) Osbeck] that differed in Al tolerance were hydroponically treated with nutrient solution (Control) or supplemented by 1.0 mM Al³⁺ (Al toxicity) for 21 days after three months of pre-culture. The Al distribution at the tissue level of citrus species following the order: lateral roots > primary roots > leaves > stems. The fragmentation of fresh lateral roots revealed the ratio of Al distribution at the cell wall, cell organelle and cytoplasmic supernatant was about 8:2:1 of two citrus species under Al stress. Besides, the Al distribution at the lateral root cell wall components suggested the pectin is the most Al-accumulating site in citrus species. Compared to *C. grandis*, *C. sinensis* had a significantly higher Al concentration on the cell wall of lateral roots whereas remarkably lower Al levels on the leaves and stems. Furthermore, the Al translocation revealed by the absorption kinetics of the cell wall demonstrated that *C. sinensis* had a higher Al retention and stronger Al affinity on the root cell wall than *C. grandis*. According to the FTIR (Fourier transform infrared spectroscopy) analysis, the Al distribution and translocation might be affected by modifying the structure and components of the citrus lateral root cell wall.

Conclusions: A higher Al-retention, mainly targeted by the pectin of the root cell wall, and a lower Al translocation efficiency from roots to shoots contributed to a higher Al tolerance of *C. sinensis* than *C. grandis*.

Background

Arable soil acidification is increasing in China from 1980s to 2000s [1]. The soil acidification accelerates aluminum (Al) solubilization from minerals significantly when the soil pH is less than 5.0 [2]. The excess Al in the soil disturbs the nutrient and water balance of the rhizosphere, reducing crop yield [3], which represented one of the most limiting factors in tropical and subtropical regions [4]. For instance, it was reported that rice grain yield decreased by 28–62% [5], and wheat grain yield decreased by 23–100% [6] under Al toxicity.

The citrus orchards in south China frequently suffer from Al toxicity induced by soil acidification [7]. For instance, our investigation on the 319 soil samples from citrus orchards in Fujian province of China revealed the tested soil samples had an average pH of 4.34 and over 90% of which had a pH lesser than 5.0 [8]. In the field condition, excess Al inhibited the root development of *Citrus aurantium* L. significantly [9]. Accordingly, the citrus fruit yield decreased significantly under Al toxicity [10]. In the sandy culture, the biomass of citrus seedlings was depressed by Al toxicity, inducing the oxidative stress and the photosynthetic inhibition of citrus seedlings [11]. Likewise, in the hydroponic culture, high Al

concentration induced chlorotic and mottled leaves, thick root tips and less fibrous roots of citrus rootstocks [12].

The plant Al tolerance mainly relied on the rejection of Al uptake and the restriction of Al translocation [13]. The Al accumulated primarily in the roots of citrus seedlings [14, 15]. Furtherly, the Al partitioning at the cellular level revealed that the plant root cell wall is the primary target for Al-binding for most crops [16]. The cell wall was constituted mainly by polysaccharides, such as pectin, cellulose and hemicellulose. However, it is still debatable which cell wall component contributed most to the Al-binding under Al stress. For instance, Yang et al. [17] reported that hemicellulose is the main pool for Al accumulation in *Arabidopsis*. Differentially, Ye et al. [18] proposed that the cell wall pectin contributed mainly to Al binding in *Panax notoginseng*, a native plant adapted to acid soil. To our knowledge, the Al distribution pattern and the primary Al target site of citrus species are still less discussed. Besides, the potential mechanisms regarding the Al distribution and translocation in citrus species are not fully documented.

We have evaluated citrus species that differed in Al tolerance at bio-physiological [12, 19], transcriptional [20] and proteomic levels [21, 22]. Our prior studies indicated *C. sinensis* is much tolerant to Al toxicity than *C. grandis*. However, potential Al-tolerant mechanisms regarding Al distribution and translocation of citrus species are less discussed. In the present study, seedlings of *C. sinensis* (much Al-tolerant) and *C. grandis* (less Al-tolerant) were cultured by hydroponics using the nutrient solution without (as of Control) or with 1.0 mM Al³⁺ (as Al toxicity). The Al distribution and translocation were investigated by cell wall fragmentation to explore the primary Al-binding site of citrus species. Besides, the study also discussed the kinetics analysis of Al adsorption and desorption, and the FTIR test of the root cell wall of two citrus species. The study will increase our understanding of the physiological mechanisms underlying the Al adaptation of citrus species.

Results

The Al distribution at the tissue level of citrus species

As shown in Fig. 1, 1.0 mM Al treatment significantly promoted Al content in lateral roots (Fig. 1a) and primary roots (Fig. 1b) compared to the Control in seedlings of two citrus species. A significant increase of Al content could also be found in the Al-treated leaves and the stems in *C. grandis* seedlings (Fig. 1c and 1d). However, no significant difference in Al content was observed in the Al-treated leaves and stems of *C. sinensis* seedlings compared to the Control. The comparison between citrus species demonstrated that the leaves and stems of *C. grandis* had remarkably higher Al content than *C. sinensis* under Al treatment. In contrast, *C. sinensis* lateral roots had a notably higher Al content than that of *C. grandis* under Al stress. Additionally, the Al content at tissue level was found to be lateral roots > primary roots > leaves > stems under Al stress.

The Al distribution at the subcellular level of citrus species

The cell wall, cell organelle and cytoplasmic supernatant of fresh lateral roots of citrus seedlings were further isolated. The Al content of each fraction was quantified respectively to investigate the Al distribution at the subcellular level (Fig. 2). The results indicated a significantly higher Al content in the Al-treated subcellular components of lateral roots than the Control in both citrus species. Strikingly, the cell wall had the most while the cytoplasmic supernatant had the most negligible Al content under Al stress of three cellular fragments. Regardless, there was no significant difference in Al content on the subcellular components of lateral roots in *C. sinensis* compared to *C. grandis* under Al stress.

The Al content of the root cell wall calculated by dry weight of citrus roots was presented in Fig. 3. The results indicated that under Al stress, the root cell wall of *C. sinensis* had a significantly higher Al than that of *C. grandis*.

The Al distribution at cell wall fragments of citrus species

The cell wall components of pectin, HC-I, HC-II and cellulose were isolated for Al quantification. The results of Fig. 4a indicated the Al content significantly increased in the pectin of the Al-treated cell wall of two citrus species. However, the Al content significantly decreased in HC-I and HC-II of *C. sinensis*. Differentially, there was no significant difference in Al content in HC-I and HC-II of *C. grandis* (Fig. 4b and 4c). In addition, the Al contents in the cellulose of two Citrus species had no remarkable difference under Al stress compared to control.

The Al adsorption and desorption analysis of root cell wall of citrus species

The cell wall of the lateral root of two citrus species was extracted for kinetics analysis of Al adsorption and desorption within 600 minutes. As shown in Fig. 5a, much Al uptake was found in the root cell wall of *C. sinensis* compared to *C. grandis*, indicating the root cell wall of *C. sinensis* had a higher capacity on Al binding than *C. grandis*. Moreover, the relative desorption rate in Fig. 5b showed that the lateral root cell wall of *C. sinensis* had a higher Al-binding rate than that of *C. grandis*. Differentially, *C. sinensis* had a lower Al desorption rate compared to *C. grandis* within 600 minutes.

The Ftir Spectra Of Lateral Root Cell Wall

The alterations of cell wall composition and structure by Al toxicity were revealed by FTIR analysis (Fig. 6). The wavenumber of spectra from two citrus species and related assignments were listed in Table 1. As found, the root cell wall of the Control from two citrus species had almost the same band position, indicating the similar composition of chemical groups of the root cell wall. However, band positions shifted under Al toxicity differentially in two citrus species. For instance, the vibration located at 3400 cm^{-1} was moved to 3396 cm^{-1} in *C. grandis* by Al toxicity. The vibration was shifted from 2856 cm^{-1} to 2858 cm^{-1} in *C. sinensis* and 2858 cm^{-1} to 2860 cm^{-1} in *C. grandis* by Al toxicity. It was also strikingly to find that most band positions from 1800 cm^{-1} to 800 cm^{-1} , representing information of characteristic polysaccharides, amide and ester, were shifted in both of two citrus species by Al toxicity.

Apart from the band position shift, the relative absorbance at most band positions was also downregulated by Al toxicity in two citrus species compared to the Control (Fig. 6a and 6b). The digital subtraction spectra were generated by minus the Al-treated spectra from the Control spectra of the cell wall of two citrus species, respectively. As found in Fig. 6c, the band intensity of the *C. grandis* was stronger than that of *C. grandis* overall. The OPLS-DA on the relative absorbance also reflected a more apparent separation between the Control and Al-toxic cell wall of *C. grandis* than *C. sinensis* (Fig. 6d).

Table 1

The infrared absorption frequencies of the cell wall and tentative assignment. Seedlings of *C. sinensis* and *C. grandis* were treated with nutrient solution (Control, pH 4.3) or supplemented by 1.0 mM Al³⁺ (1.0 mM Al toxicity, pH 4.3). The lateral root cell wall samples were extracted for FTIR spectra analysis.

Wavenumber (cm ⁻¹)				Tentative Assignment	Reference
C. sinensis		C. grandis			
Control	Al toxicity	Control	Al toxicity		
3400	3400	3400	3396	OH stretching	[43]
2924	2926	2924	2926	CH asymmetric stretching	[44]
2856	2858	2858	2860	CH symmetric stretching	[44]
1740	1740	1740	1740	C = O stretching of ester	[44]
1649	1649	1649	1649	C = O stretching of amide I band	[45]
1545	1543	1543	1543	NH bending and CN stretching of amide II band	[45]
1514	1518	1520	1520	NH bending and CN stretching of amide II band	[46]
1427	1427	1427	1427	CH ₂ symmetric deformation	[47]
1375	1375	1373	1373	COO- symmetric stretching and aliphatic group vibration	[48]
1329	1331	1327	1331	C-O	[49]
1246	1244	1246	1244	C = O stretching or NH bending of amide III bands	[47]
1155	1153	1153	1153	phosphoryl group	[44]
1103	1101	1103	1105	C = O stretching, alcohol hydroxyl, ether or ester base	[45]
1059	1047	1059	1054	C-OH stretching of alcoholic groups and carboxylic acids	[50]
899	-	899	906	β-linkage between two glucose units	[47]

Discussion

The citrus fruit trees are superbly adapted to the acid soil with potential high Al in south China [23]. Understanding of Al partition and mobilization *in vivo* is pivotal to reveal the Al tolerance of citrus species. Besides, it is of great significance to disclose the Al binding site of citrus species for Al toxicity mitigation. The present study addressed both challenges. The hydroponic culture had been widely carried out to explore the ion behavior of citrus species [24, 25]. Compared to our previous study in sandy culture with 1.0 mM Al treated for 18 weeks [20], the present 21 days' hydroponic culture of citrus species resulted in almost the same Al level in leaves, indicating a reliable treatment of the study.

It has been evidenced that Al-induced phytotoxicity has many target sites from the apoplast to symplast in higher plants [26]. Accordingly, plant species varied in Al-tolerance have evolved different strategies to cope with Al toxicity based on Al distribution and translocation. Plant species native to acid soils are often found to retain excess Al in insensitive roots, protecting leaves from metabolic disruption [27]. For instance, Kopittke et al. [13] reported that the Al-tolerant wheat accumulated more than four times of Al in roots compared to the sensitive line. Similarly, the higher Al content on the root apex was also observed in Al-tolerant common bean compared to the Al-sensitive genotype [28]. The present results supported higher Al in roots under Al stress compared to shoots in citrus species (Fig. 1). Besides, *C. sinensis* had a significantly higher Al content in lateral roots but significantly lower Al content in shoots than *C. grandis* under Al stress. Thus, the less Al translocation from roots to shoots in *C. sinensis* might contribute to the mitigation of Al-toxicity in the shoot. Likewise, the higher Al translocation of *C. grandis* than *C. sinensis* was also reported in our previous study by 1.0 mM Al stress under 18 weeks' sandy culture [12]. However, the Al stress within 21 days did not significantly differ in the biomass accumulation of two citrus species (data not shown). With the stress duration increased to 15 weeks, the *C. sinensis* seedlings had remarkably higher biomass accumulation than *C. grandis* in both leaves and roots (Fig. s1). Conclusively, the relatively higher Al tolerance of *C. sinensis* is related to a less Al translocation from the roots to shoots.

Plant root cell wall is the first defense conferring Al toxicity. Clarkson et al. [29] revealed that over 85% of Al accumulated on the cell wall of barley roots. For woody plants, more than 88% of total Al was localized in the root cell wall of the conifer [30]. In the study, the cell wall of citrus lateral roots accumulates higher Al content than the cell organelle and cytoplasmic supernatant. The ratio of Al concentration on the cell wall, cell organelle and cytoplasmic supernatant is about 8:2:1 (Fig. 2a) under 1.0 mM Al stress, indicating the prominent roles of the root cell wall in Al immobilization of citrus species. Interestingly, the ratio of cell wall-binding Al is very close to the finding of Al-treated tea (*Camellia sinensis*) roots [31]. Moreover, the Al distribution at cell wall fraction is in the order of pectin > HC-II > HC-I > cellulose, suggesting the pectin holds the most while the cellulose has the least Al. The contribution of pectin in Al sequestration was also reported in rice roots [32]. Li et al. [33] proposed that a high density of carboxylic groups on the pectin contributes to Al binding. Further studies regarding pectin content and related structural deformation under Al stress of citrus species are needed to reveal the role of pectin in Al detoxification.

Ma et al. [34] reported that the cell wall of Al sensitive wheat had higher Al retention than Al tolerant cultivar under 10 μM Al within 9 hours' duration. By contrast, we observe that dry roots of *C. sinensis* had a remarkably higher Al content on the cell wall than that of *C. grandis* (Fig. 3), which is consistent with the higher Al content of lateral roots in *C. sinensis* than *C. grandis*. Therefore, we propose that the Al distribution pattern in higher plants depends on the toxic intensity, such as Al level and stress duration. For example, the Al tolerant cultivar might exclude Al encountering weak Al stress, which resulted in less Al accumulation. However, when the Al exclusion is not enough for Al detoxification, the mechanism of Al translocation *in vivo* was activated, such as Al stabilization on the roots or cell wall. For another, the Al distribution and translocation might reflect the flexible strategies for Al detoxification between woody and gramineous plants considering the different root structures and extreme variation of root biomass.

The adsorption and desorption kinetics demonstrated that the root cell wall of *C. sinensis*, an Al-tolerant species, had a higher Al affinity than *C. grandis* (Fig. 5). By contrast, the root cell wall of *C. grandis* exhibited a lower Al adsorption and a higher Al desorption, indicating less tight Al-binding on the root cell wall, which would facilitate higher Al translocation from apoplast to symplast. Therefore, we infer that Al-tolerant woody plants were prone to retain excess Al on the root cell wall to diminish Al translocation owing to their high capacity of the root systems. Besides, the Al binding firmly on roots is economical for Al resistance considering the energy cost during Al translocation. The findings of the present results also implied that organic material prepared from cell walls is promising in alleviating the Al toxicity of the citrus plants in acidic red soils.

The Al binding resulted in modification of the root cell wall, which could be assessed by FTIR analysis [35, 36]. In the study, the results that almost no new characteristic peak emerged indicated less effect of Al toxicity on the types of functional groups on the cell wall by Al toxicity overall in two citrus species. The modification of cell wall by Al stress might mainly be dependent on the abundance of chemical groups on the root cell wall of citrus species. For instance, the spectra at 3400 cm^{-1} (-OH stretching), was shifted to 3396 cm^{-1} under Al stress in *C. grandis*, suggesting the changed hydrogen-bonding mode and the destroyed connection of cell wall components by Al toxicity (Table 1). The results approved less Al tolerance of *C. grandis* than *C. sinensis* by considering the flexible deformation of hydrogen bonds between molecules [24]. Also, a study indicated the absorbance at 1740 and 1649 cm^{-1} represents the absorption of the esterified and non-esterified carboxyl groups of pectin, respectively [37]. The present results of downregulated relative absorbance at 1740 cm^{-1} and 1649 cm^{-1} were coincident with significantly higher Al accumulation in the pectin (Fig. 6c), suggesting the role of cell wall pectin in Al-binding under Al toxicity. Besides, it is also interesting to find that the vibrations from 1200 cm^{-1} to 900 cm^{-1} (Table 1), which belong to the polysaccharide fingerprint region [38], shifted and decreased under Al toxicity. The results indicated that the altered structure and content of cell wall polysaccharides under Al toxicity would affect the Al binding on the root of citrus species. Both of the digital subtraction spectra (Fig. 6c) and the OPLS-DA (Fig. 6c) of relative absorbance in two citrus species supported a much apparent alteration of the cell wall in *C. grandis* compared to *C. sinensis*, such as severer damage under Al toxicity. Similarly, a higher relative absorbance of the upper leaves corresponding to a much obvious

symptom of boron deficient orange seedlings compared to lower leaves was also reported based on the FTIR analysis [24]. Further studies based on isotope labeling of Al and pectin deformation and polysaccharides quantification of the citrus root cell wall are needed to disclose the Al spatial and temporal distribution.

Conclusion

The study indicated that Al toxicity altered the structure and components of the root cell wall in citrus seedlings. The pectin of the lateral root cell wall was most abundant in the Al-accumulation of citrus species. Compared to *C. grandis*, a less tolerant citrus species, *C. sinensis* had a higher Al retention on the root cell wall and a lower Al translocation efficiency from roots to shoots by 1.0 mM Al treated for 21 days in hydroponics. The novel mechanisms in Al partition and translocation could be crucial for citrus seedlings to cope with Al toxicity.

Methods

Plant culture and treatments

The citrus species 'Xuegan' [*Citrus sinensis* (L.) Osbeck] and 'Suanyou' [*Citrus grandis* (L.) Osbeck] used in the study were formally identified by Fujian Academy of Forestry Sciences (FAFS, Fuzhou, China). In December 2018, citrus fruits were harvested from the demonstration orchard of FAFS and stored in a fridge at 4 °C. For germination, the seeds of *C. sinensis* and *C. grandis* were sown in a plastic tray filled with clean river sand at the greenhouse in early April of 2019. Four weeks after germination, seedlings of uniform size (about 10 cm) were transferred to black tanks containing nutrient solution and aerated for 30 min every two hours. The nutrient solution contained 1 mM KNO₃, 1 mM Ca(NO₃)₂, 0.1 mM KH₂PO₄, 0.5 mM MgSO₄, 10 μM H₃BO₃, 2 μM MnCl₂, 2 μM ZnSO₄, 0.5 μM CuSO₄, 0.065 μM (NH₄)Mo₇O₂₄ and 20 μM Fe-EDTA. The pH of the nutrient solution was adjusted to 4.30 by 1 M HCl or NaOH and was replaced every two days. Three months after transplanting, the plants were subjected to the treatments with 0 (Control) or 1.0 mM Al (Al toxicity) in the nutrient solution described above (pH 4.30). The samples of citrus leaves, stems, primary roots and lateral roots were divided and collected 21 days after treatments when visible leaf chlorosis appeared on Al-treated *C. grandis* leaves.

Quantification Of Al At The Tissue Level

The leaves, stems, primary roots and lateral roots of citrus species were dried and digested in HNO₃/HClO₄ (5:1, v/v), and Al content was quantified according to Hsu [39].

Quantification of Al on the cell wall, cell organelle and cytoplasmic supernatant of fresh lateral roots

The cell wall, cell organelle and cytoplasmic supernatant were isolated according to Gao et al. [40]. In brief, 0.3 g of fresh citrus lateral roots was homogenized with buffer containing 0.25 M sucrose, 50 mM

Tris-HCl (pH7.5) and 1 mM dithiothreitol at 4°C. The homogenate was then filtered through an 8-layer of cheesecloth to collect the filtrate 1. Then the residue left on the cheesecloth was washed twice by the buffer described above to get the filtrate 2. Both filtrate 1 and filtrate 2 were pooled and centrifuged at 300 g for 30 s. The resulting pellet after centrifugation and the residue on the cheesecloth were pooled as the cell wall debris. Meanwhile, the harvested supernatant was further centrifuged at 20,000 g for 45 min to obtain the cytoplasmic supernatant on the top and the cell organelle at the sediments. Finally, the samples of subcellular components were digested by 6 ml of HNO₃: HClO₄ (1:5, v/v) overnight and quantified by ICP-MS.

Quantification of Al on cell wall fractions of citrus lateral roots

The crude cell wall of citrus lateral roots was extracted and fractioned according to Zhong and Lauchli [41] with modifications. Briefly, about 50 mg citrus lateral root was powdered and pooled into a centrifuge tube with 5 ml ice-cold 75% ethanol for 20 min on ice. The samples were then centrifuged at 1000 g for 10 min. The supernatant was discarded, and the resulted pellets were centrifugated at 17,000 g for 10 min three times with 5 ml 80% ethanol, methanol-chloroform mixture (1:1, v/v) and acetone, respectively. The final pellets were pooled as crude cell wall after dried and weighted.

The dry crude cell wall from the lateral roots of citrus seedlings was added into ammonium oxalate (containing 0.1% NaBH₄, pH = 4.0) (5 mg cell wall/1ml solution) in a boiling water bath for one hour and centrifuged at 17,000 g for 10 min for three times to isolate the pectin, hemicellulose 1 (HC-I), hemicellulose 2 (HC-II) and cellulose. After centrifugation, the supernatants of each were pooled and collected as cell wall pectin. The residue was washed by water twice then extracted by 4% KOH (containing 0.1% NaBH₄) or 24 % KOH (containing 0.1% NaBH₄) under room temperature three times for 24 h in total subsequently. The obtained supernatant was HC-I and HC-II fractions, respectively. The debris left was pooled as cellulose. The volume of cell wall components was measured and stored at 4 °C. The Al content of the cell wall and each cell wall component was quantified according to the method described above.

Al Adsorption And Desorption Kinetics

The Al adsorption and desorption kinetics were performed according to Zheng et al. [42] with modifications. Briefly, the adsorption solution of 0.5 mM Al³⁺ in 0.5 mM CaCl₂ (pH 4.30) was pumped by a peristaltic pump at 0.2 ml/min through a 2 ml column loaded with 10 mg root cell wall for Al adsorption. The solution after cell wall adsorption was then collected by a fraction collector at 20 min intervals until the Al content was equal to the adsorption solution. The residue Al³⁺ left in the system was washed by 0.5 mM CaCl₂ (pH 4.5) at 0.6 ml/h for 1 h before Al desorption by 2.5 mM CaCl₂ (pH 4.30) at 0.2 ml/h until the Al concentration in the collector below detection limit. Finally, the Al content in the fraction collector was quantified, and the kinetics were analyzed within 600 min. The Al absorption and desorption kinetics were performed three times independently.

FTIR spectra analysis

2 mg dry cell wall of Citrus lateral root was mixed with 200 mg KBr and pressed into a disk by FW-5A Pressor. The IR spectra of cell walls ranging from 4000 – 400 cm^{-1} were recorded using Vertex 70 spectrometer with a resolution of 4 cm^{-1} and 32 scans per sample. The obtained spectra were normalized and baseline-corrected by OPUS management software before exported to Excel. The data of FTIR spectra were processed by Origin Pro 2020b (OriginLab Corporation, USA). The OPLS-DA (orthogonal partial least-squares discrimination analysis) was performed in SIMCA 14.1 (Umetrics AB, Umea, Sweden).

Data Analysis

Data analysis was performed by two-way analysis of variance, and significant differences ($P < 0.05$) among treatments were statistically evaluated by Two-Way ANOVA using Duncan's test, using the SPSS 16.0 (SPSS Corp., Chicago, IL, USA). All the values are presented as means \pm SE. Figures except OPLS-DA were generated by using Sigmaplot 12.0.

Abbreviations

HC: hemicellulose;

Declarations

Ethics approval and consent to participate

Not applicable.

Consent for publication

Not applicable.

Availability of data and materials

The datasets used and/or analysed during the current study are available from the corresponding author on reasonable request.

Competing interests

The authors declare that they have no competing interests

Funding

This research was funded by the National Natural Science Foundation of China (31801950) and the Special Fund for Scientific and Technological Innovation of Fujian Agriculture and Forestry University (CXZX2019079S). The funders had no role in the design of the study and collection, analysis, and interpretation of data and in writing the manuscript.

Authors' contributions

HZ wrote the manuscript; XL analyzed the experimental results; ML prepared the figures and tables; PH carried out the experiments; NL designed the experiment; ZH revised the drafts of the manuscript; LC reviewed drafts of the manuscript. All authors read and approved the final manuscript.

Acknowledgments

Not Applicable.

Authors' information

¹ College of Resources and Environment, Fujian Agriculture and Forestry University, Fuzhou 350002, China; ² College of Forestry, Guangxi University, Nanning 530004, China;

References

1. Guo JH, Liu XJ, Zhang Y, Shen JL, Han WX, Zhang WF, Christie P, Goulding KWT, Vitousek PM, Zhagn FS. Significant acidification in major Chinese croplands. *Science*. 2010;327(5968):1008–10.
2. Lindsay WL, Walthall PM. The solubility of aluminum in soils. In: *The environmental chemistry of aluminum*. Boca Raton: CRC Press; 2020. pp. 333–61.
3. Li J, Su L, Lv A, Li Y, Zhou P, An Y. MsPG1 alleviated aluminum-induced inhibition of root growth by decreasing aluminum accumulation and increasing porosity and extensibility of cell walls in alfalfa (*Medicago sativa*). *Environ Exp Bot*. 2020;175:104045.
4. Xia H, Riaz M, Zhang M, Liu B, El-Desouki Z, Jiang CC. Biochar increases nitrogen use efficiency of maize by relieving aluminum toxicity and improving soil quality in acidic soil. *Ecotox Environ Safe*. 2020;196:110531.
5. Kang DJ, Seo YJ, Futakuchi K, Vijarnsorn P, Ishii R. Effect of aluminum toxicity on flowering time and grain yield on rice genotypes differing in Al – tolerance. *J Crop Sci Biotech*. 2011;14(4):305–9.
6. Valle SR, Carrasco J, Pinochet D, Calderini DF. Grain yield, above-ground and root biomass of Al – tolerant and Al – sensitive wheat cultivars under different soil aluminum concentrations at field conditions. *Plant Soil*. 2009;318:299–310.
7. Yan L, Riaz M, Wu XW, Du CQ, Liu YL, Jiang CC. Ameliorative effects of boron on aluminum induced variations of cell wall cellulose and pectin components in trifoliolate orange (*Poncirus trifoliolate* (L.) Raf.) rootstock. *Environ Pollu*. 2018;240:764–74.

8. Li Y, Han MQ, Lin F, Ten Y, Lin J, Zhu DH, Guo P, Weng YB, Chen LS. Soil chemical properties, Guanximiyou pummelo leaf mineral nutrient status and fruit quality in the southern region of Fujian province, China. *J Soil Sci Plant Nut.* 2015;15(3):615–28.
9. Lin ZY, Myhre DL. Citrus root growth as affected by soil aluminum level under field conditions. *Soil Sci Soc Am J.* 1990;54(5):1340–4.
10. Li D, Li X, Han QZ, Zhou YZ, Dong JL, Duan ZQ. Phosphorus application improved the yield of citrus plants grown for three years in an acid soil in the three gorges reservoir area. *Sci Hortic.* 2020;273:109596.
11. Guo P, Qi YP, Cai YT, Yang TY, Yang LT, Huang ZR, Chen LS. Aluminum effects on photosynthesis, reactive oxygen species and methylglyoxal detoxification in two citrus species differing in aluminum tolerance. *Tree Physiol.* 2018;38(10):1548–65.
12. Silva CM, Cavalheiro MF, Bressan ACG, Carvalho BMO, Banhos OFAA, Purgatto E, Harakava R, Tanaka FAO, Habermann G. Aluminum-induced high IAA concentration may explain the Al susceptibility in *Citrus limonia*. *Plant Growth Regul.* 2019;87(1):123–37.
13. Kopittke PM, McKenna BA, Karunakaran C, Dynes JJ, Arthur Z, Gianoncelli A, Kourousias G, Menzies NW, Ryan PR, Wang P. Aluminum complexation with malate within the root apoplast differs between aluminum resistant and sensitive wheat lines. *Front Plant Sci.* 2017;8:1377.
14. Chen LS, Yang LT, Guo P, Jiang HX, Tang N. Aluminum toxicity and fruit nutrition. In: *Fruit Crops.* Elsevier. 2020.p.223–240.
15. Yang TY, Qi YP, Huang HY, Wu FL, Huang WT, Deng CL, Yang LT, Chen LS. Interactive effects of pH and aluminum on the secretion of organic acid anions by roots and related metabolic factors in *Citrus sinensis* roots and leaves. *Environ Pollut.* 2020;262:114303.
16. Li CX, Yan JY, Ren JY, Sun L, Xu C, Li GX, Ding ZJ, Zheng SJ. A WRKY transcription factor confers aluminum tolerance via regulation of cell wall modifying genes. *J Integ Plant Biol.* 2020;62(8):1176–92.
17. Yang JL, Zhu XF, Peng YX, Zheng C, Li GX, Liu Y, Shi YZ, Zheng SJ. Cell wall hemicellulose contributes significantly to Al adsorption and root growth in *Arabidopsis*. *Plant Physiol.* 2011;155(4):1885–92.
18. Ye Yang, Dai C, Gu L, Qu Y, Yang X, Chen Q, Liu D, Wang C, Cui X. Distribution pattern of aluminum in *Panax notoginseng*, a native medicinal plant adapted to acidic red soils. *Plant Soil.* 2018;423(1):375–84.
19. Yang LT, Jiang HX, Qi YP, Chen LS. Differential expression of genes involved in alternative glycolytic pathways, phosphorus scavenging and recycling in response to aluminum and phosphorus interactions in citrus roots. *Mol Biol Rep.* 2012;39(5):6353–66.
20. Guo P, Qi YP, Yang LT, Lai NW, Ye X, Yang Y, Chen LS. Root adaptive responses to aluminum-treatment revealed by RNA-Seq in two citrus species with different aluminum-tolerance. *Front Plant Sci.* 2017;8:330.

21. Jiang HX, Yang LT, Qi YP, Lu YB, Huang ZR, Chen LS. Root iTRAQ protein profile analysis of two citrus species differing in aluminum-tolerance in response to long-term aluminum-toxicity. *BMC Genom.* 2015;16:949.
22. Li H, Yang LT, Qi YP, Guo P, Lu YB, Chen LS. Aluminum toxicity-induced alterations of leaf proteome in two citrus species differing in aluminum tolerance. *Int J Mol Sci.* 2016;17(7):1180.
23. Zhang H, Li XY, Chen LS, Huang ZR. The photosynthetic performance of two citrus species under long-term aluminum treatment. *Photosynthetica.* 2020;58(2):228–35.
24. Liu GD, Dong XC, Liu LC, Wu LS, Jiang CC. Boron deficiency is correlated with changes in cell wall structure that lead to growth defects in the leaves of navel orange plants. *Sci Hortic.* 2014;176:54–62.
25. Yan L, Riaz M, Wu X, Du CQ, Liu YL, Lv B, Jiang CC. Boron inhibits aluminum-induced toxicity to citrus by stimulating antioxidant enzyme activity. *J Environ Sci Heal C.* 2018;36(3):145–63.
26. Zheng SJ, Yang JL. Target sites of aluminum phytotoxicity. *Biol Plantarum.* 2005;49(3):321–31.
27. Watanabe T, Osaki M. Mechanisms of adaptation to high aluminum condition in native plant species growing in acid soils: a review. *Commun Soil Sci Plan.* 2002;33:1247–60.
28. Rangel AF, Rao IM, Horst WJ. Intracellular distribution and binding state of aluminum in root apices of two common bean (*Phaseolus vulgaris*) genotypes in relation to Al toxicity. *Physiol Plantarum.* 2009;135(2):162–73.
29. Clarkson DT. Interactions between aluminium and phosphorus on root surfaces and cell wall material. *Plant Soil.* 1967;27(3):347–56.
30. Heim A, Brunner I, Frey B, Frossard E, Luster J. Root exudation, organic acids, and element distribution in roots of Norway spruce seedlings treated with aluminum in hydroponics. *J Plant Nutr Soil Sc.* 2001;164(5):519–26.
31. Hajiboland R, Bastani S, Bahrami-Rad S, Poschenrieder C. Interactions between aluminum and boron in tea (*Camellia sinensis*) plants. *Acta Physiol Plant.* 2015;37:54.
32. Nagayama T, Nakamura A, Yamaji N, Satoh S, Furukawa J, Iwai H. Changes in the distribution of pectin in root border cells under aluminum stress. *Front Plant Sci.* 2019;10:1216.
33. Li XW, Li YL, Qu M, Xiao HD, Feng YM, Liu JY, Wu LS, Yu M. Cell wall pectin and its methyl-esterification in transition zone determine Al resistance in cultivars of pea (*Pisum sativum*). *Front Plant Sci.* 2016;7:39.
34. Ma JF, Shen RF, Nagao S, Tanimoto E. Aluminum targets elongating cells by reducing cell wall extensibility in wheat roots. *Plant Cell Physiol.* 2004;45(5):583–9.
35. McCann MC, Chen L, Roberts K, Kemsley EK, Sene C, Carpita NC, Stacey NJ, Wilson RH. Infrared microspectroscopy: sampling heterogeneity in plant cell wall composition and architecture. *Physiol Plantarum.* 1997;100(3):729–38.
36. Chen L, Carpita NC, Reiter WD, Wilson RH, Jeffries C, McCann MC. A rapid method to screen for cell-wall mutants using discriminant analysis of Fourier transform infrared spectra. *Plant J Mol Biol.*

- 1998;16(3):385–92.
37. Chatjigakis AK, Pappas C, Proxenia N, Kalantzi O, Rodis P, Polissiou M. FTIR spectroscopic determination of the degree of esterification of cell wall pectins from stored peaches and correlation to textural changes. *Carbohydr Polym.* 1998;37(4):395–408.
 38. Barron C, Parker ML, Mills E, Rouau X, Wilson RH. FTIR imaging of wheat endosperm cell walls in situ reveals compositional and architectural heterogeneity related to grain hardness. *Planta.* 2005;220(5):667–77.
 39. Hsu PH. Effect of initial pH, phosphate, and silicate on the determination of aluminum with aluminon. *Soil Sci.* 1963;96(4):230–8.
 40. Gao HJ, Zhao Q, Zhang XC, Wan XC, Mao JD. Localization of fluoride and aluminum in subcellular fractions of tea leaves and roots. *J Agr Food Chem.* 2014;62(10):2313–9.
 41. Zhong HL, Lauchli A. Changes of cell wall composition and polymer size in primary roots of cotton seedlings under high salinity. *J Exp Bot.* 1993;44(261):773–8.
 42. Zheng SJ, Lin X, Yang J, Liu Q, Tang C. The kinetics of aluminum adsorption and desorption by root cell walls of an aluminum resistant wheat (*Triticum aestivum* L.) cultivar. *Plant Soil.* 2004;261(1):85–90.
 43. Iqbal M, Saeed A, Zafar SI. FTIR spectrophotometry, kinetics and adsorption isotherms modeling, ion exchange, and EDX analysis for understanding the mechanism of Cd²⁺ and Pb²⁺ removal by mango peel waste. *J Hazard Mater.* 2009;164(1):161–71.
 44. Chen SH, Cheow YL, Ng SL, Ting ASY. Mechanisms for metal removal established via electron microscopy and spectroscopy: a case study on metal tolerant fungi *Penicillium simplicissimum*. *J Hazard Mater.* 2019;362:394–402.
 45. Deng PY, Liu W, Zeng BQ, Qiu YK, Li LS. Sorption of heavy metals from aqueous solution by dehydrated powders of aquatic plants. *Int J Environ Sci Te.* 2013;10(3):559–66.
 46. Sigee DC, Dean A, Levado E, Tobin MJ. Fourier – transform infrared spectroscopy of *Pediastrum duplex*: characterization of a micro – population isolated from a eutrophic lake. *Eur J Phycol.* 2002;37:19–26.
 47. Abidi N, Hequet E, Cabrales L, Gannaway J, Wilkins T, Wells LW. Evaluating cell wall structure and composition of developing cotton fibers using Fourier transform infrared spectroscopy and thermogravimetric analysis. *J Appl Polym Sci.* 2008;107(1):476–86.
 48. Farinella NV, Matos GD, Arruda MAZ. Grape bagasse as a potential biosorbent of metals in effluent treatments. *Bioresource Technol.* 2007;98(10):1940–6.
 49. Saha PD, Chakraborty S, Chowdhury S. Batch and continuous (fixed – bed column) biosorption of crystal violet by *Artocarpus heterophyllus* (jackfruit) leaf powder. *Colloids Surface B.* 2012;92:262–70.
 50. Guibaud G, Tixier N, Bouju A, Baudu M. Relation between extracellular polymers' composition and its ability to complex Cd, Cu and Pb. *Chemosphere.* 2003;52(10):1701–10.

Figures

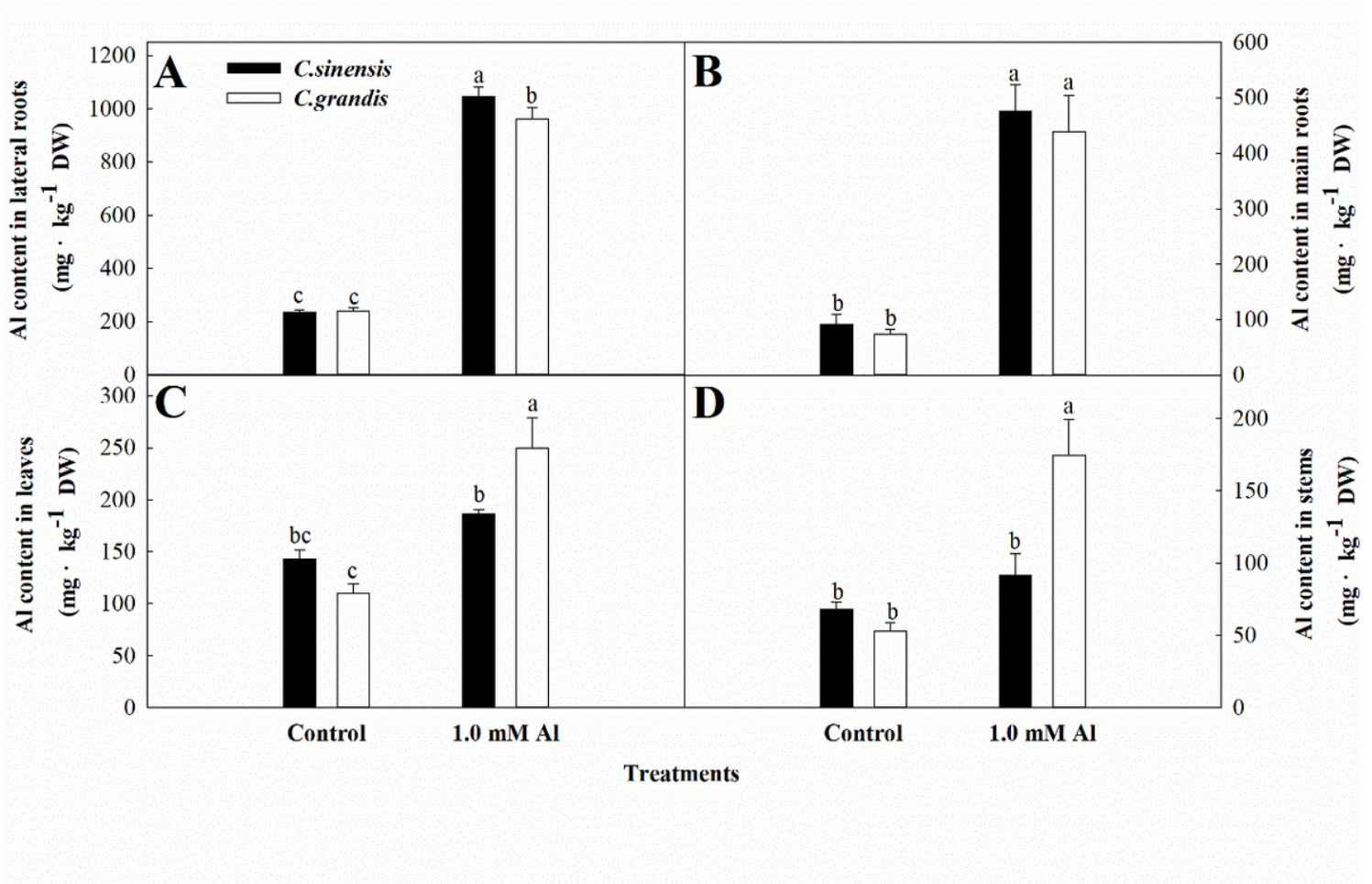


Figure 1

The effects of Al toxicity on Al distribution in lateral roots (A), primary roots (B), leaves (C) and stems (D) of *C. sinensis* and *C. grandis* seedlings. Seedlings of *C. sinensis* and *C. grandis* were treated with nutrient solution (Control, pH 4.3) or supplemented by 1.0 mM Al³⁺ (1.0 mM Al toxicity, pH 4.3) for 21 days. The values represent mean ± SE (N = 5). Significant differences (p ≤ 0.05) between treatments are indicated by different letters.

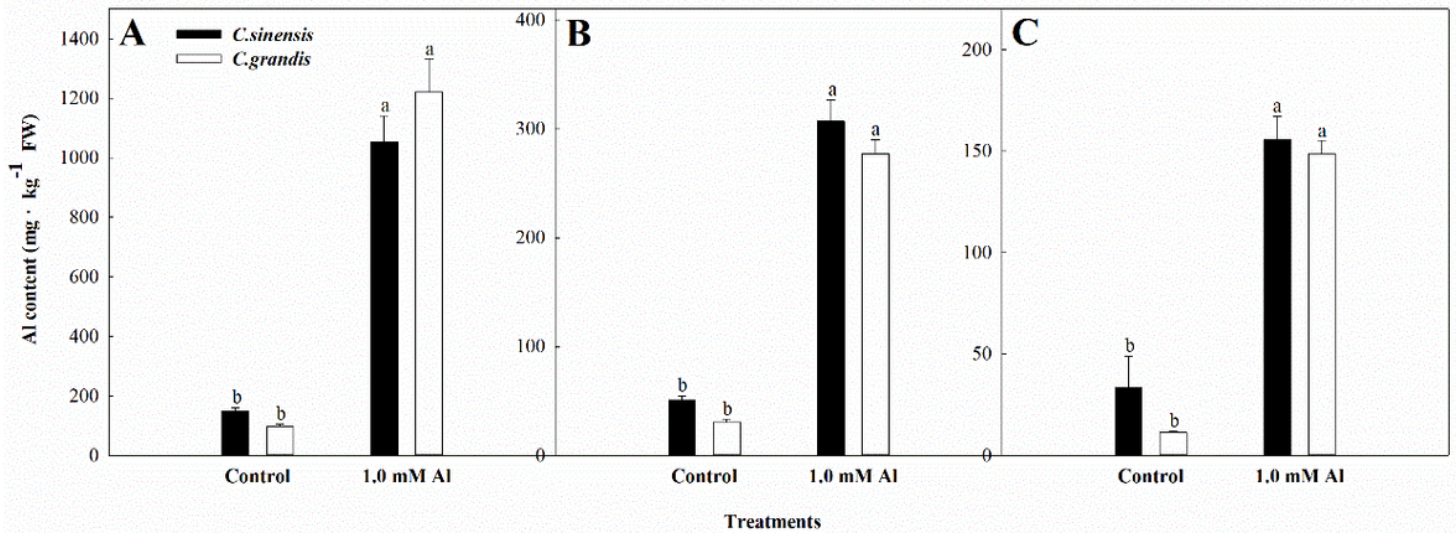


Figure 2

The Al distribution in the lateral root cell wall (A), cell organelle (B) and cytoplasmic supernatant (C) of *C. sinensis* and *C. grandis* seedlings. Seedlings of *C. sinensis* and *C. grandis* were treated with nutrient solution (Control, pH 4.3) or supplemented by 1.0 mM Al³⁺ (1.0 mM Al toxicity, pH 4.3) for 21 days. Fresh lateral roots were used for Al quantification at subcellular levels. The values represent mean ± SE (N = 5). Significant differences ($p \leq 0.05$) between treatments are indicated by different letters.

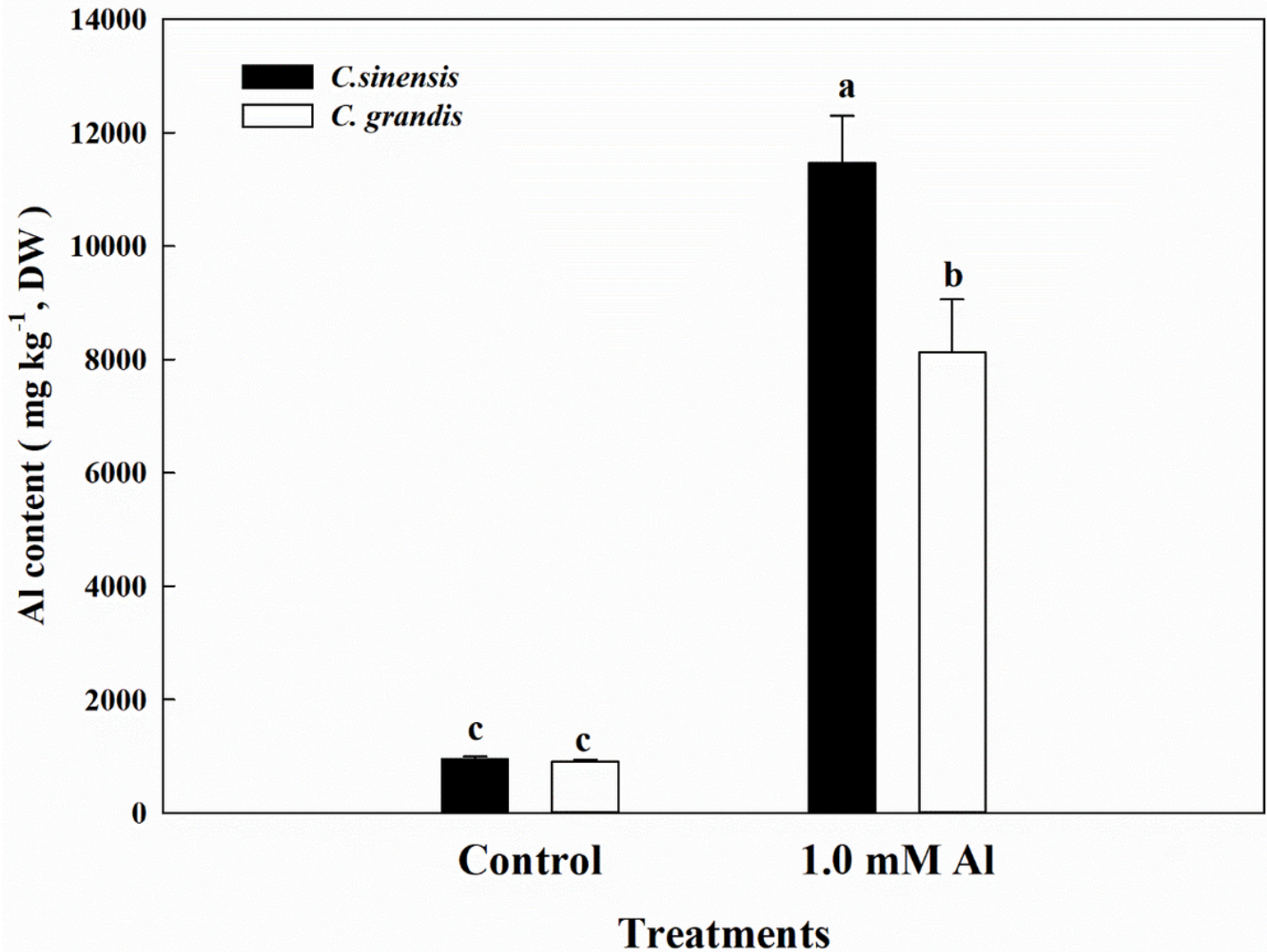


Figure 3

The effects of Al toxicity on cell wall Al contents of the dry root of *C. sinensis* and *C. grandis* seedlings. Seedlings of *C. sinensis* and *C. grandis* were treated with nutrient solution (Control, pH 4.3) or supplemented by 1.0 mM Al³⁺ (1.0 mM Al toxicity, pH 4.3) for 21 days. Dry lateral roots were used for cell wall extraction and Al quantification. The values represent mean \pm SE (N = 5). Significant differences ($p \leq 0.05$) between treatments are indicated by different letters.

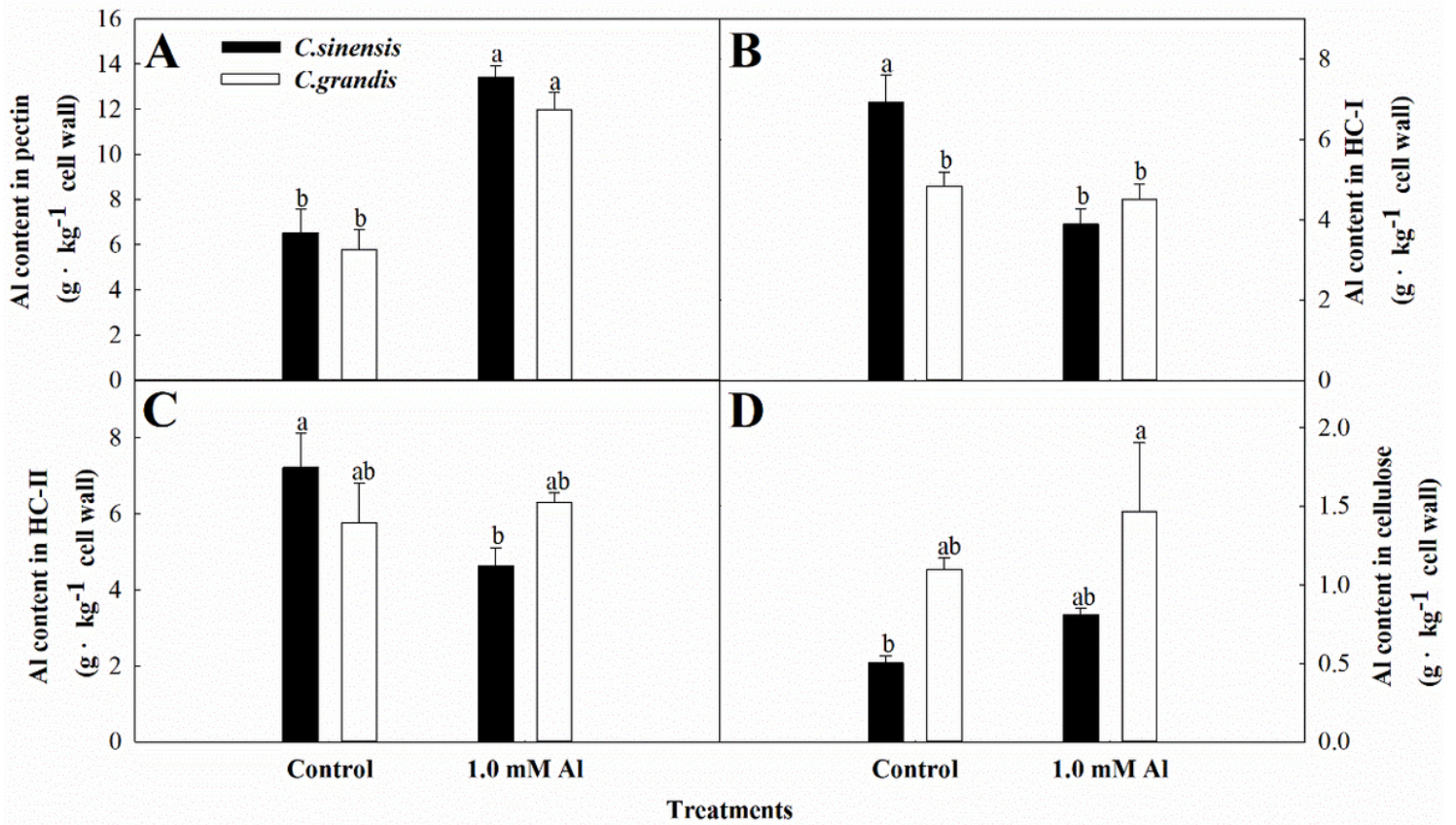


Figure 4

The Al contents on pectin (A), HC-I (B) HC-II (C) and cellulose (D) of lateral root cell wall of *C. sinensis* and *C. grandis* seedlings. Seedlings of *C. sinensis* and *C. grandis* were treated with nutrient solution (Control, pH 4.3) or supplemented by 1.0 mM Al³⁺ (1.0 mM Al toxicity, pH 4.3) for 21 days. The cell wall samples of lateral roots were fractionated for Al quantification. The values represent mean ± SE (N = 5). Significant differences ($p \leq 0.05$) between treatments are indicated by different letters.

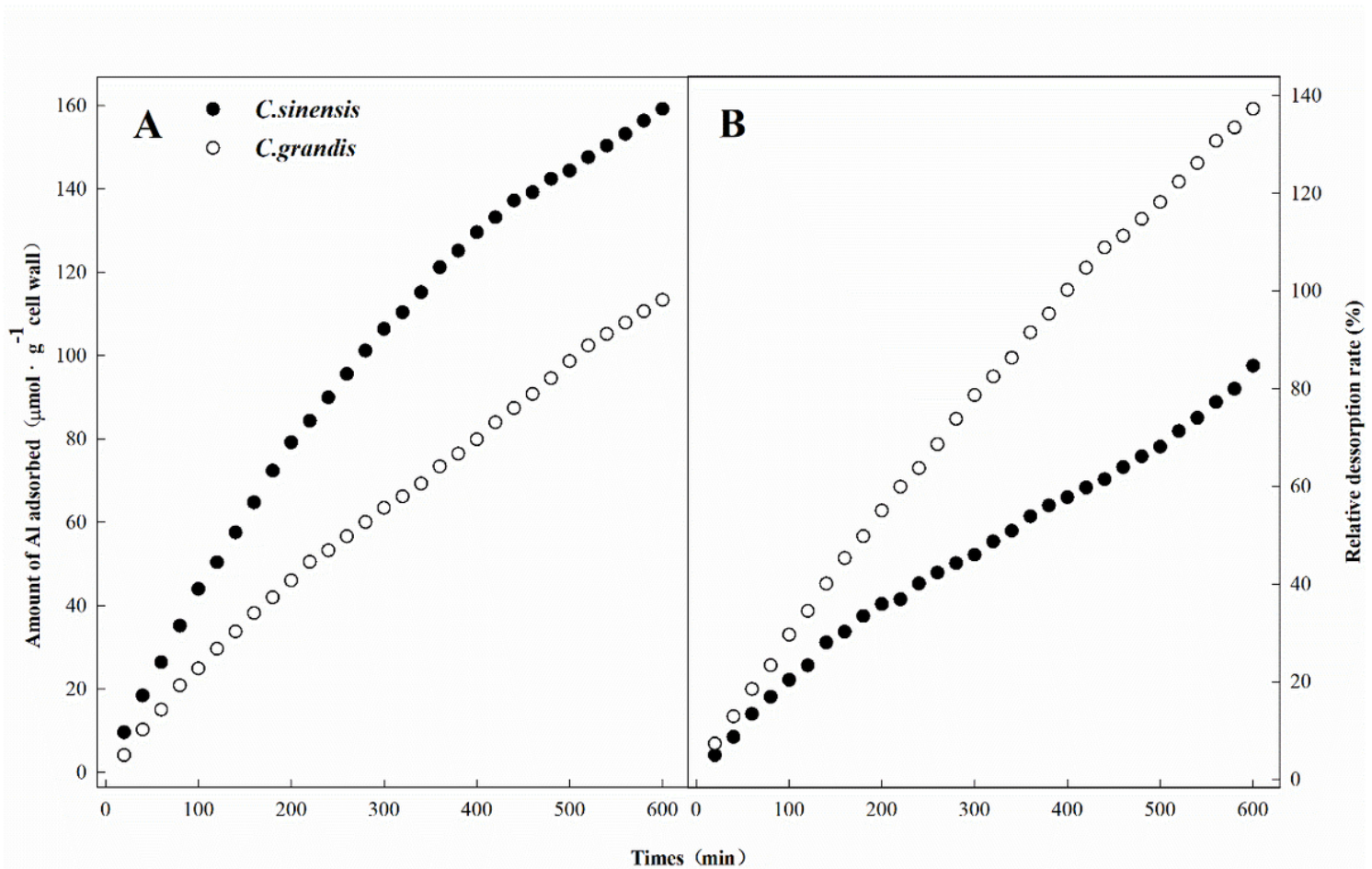


Figure 5

The Al Adsorption (A) and desorption (B) kinetics of lateral root cell wall of *C. sinensis* and *C. grandis*. Seedlings of *C. sinensis* and *C. grandis* were treated with nutrient solution (Control, pH 4.3) for 21 days. The lateral root cell wall samples were extracted for Al adsorption and desorption kinetics analysis within 600 minutes.

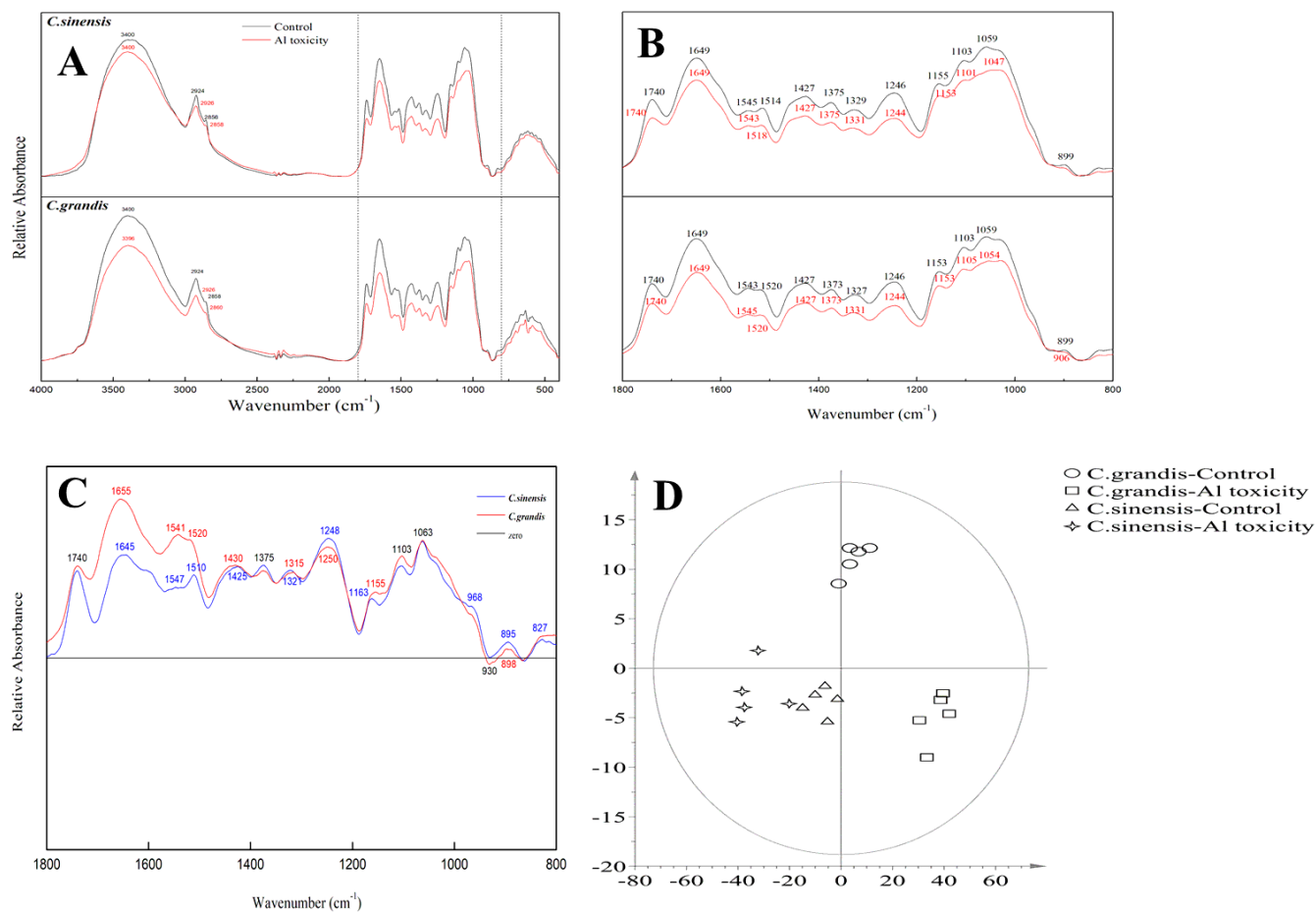


Figure 6

The FTIR spectra of the lateral root cell wall in the region of 4000 – 500 cm⁻¹ (A), 1800 – 800 cm⁻¹ (B), digital subtraction spectra (C) and the OPLS-DA of relative absorbance (D) of two citrus species. Seedlings of *C. sinensis* and *C. grandis* were treated with nutrient solution (Control, pH 4.3) or supplemented by 1.0 mM Al³⁺ (1.0 mM Al toxicity, pH 4.3). The lateral root cell wall samples were extracted for FTIR spectra analysis. The digital spectra represent Control cell wall minus Al toxic-cell wall. The values represent mean ± SE (N = 5).

Supplementary Files

This is a list of supplementary files associated with this preprint. Click to download.

- [FigureS1.pdf](#)